European Journal of Chemistry

Synthesis, spectral characterization, antimicrobial, DNA binding and antioxidant studies of Co(II), Ni(II), Cu(II) and Zn(II) metal complexes of novel thiosalen analog N2S2

Sabry Hamed Seda [1,2] and Ayman Ahmed Abdel Aziz [1,3,*]

[1] *Department of Chemistry, Faculty of Science, University of Tabuk, 71491, Tabuk, Saudi Arabia*
[2] *Department of Chemistry, Faculty of Science, Benha University, 13511, Benha, Egypt*
[3] *Department of Chemistry, Faculty of Science, Ain Shams University, Abassia, 11566, Cairo, Egypt*

* Corresponding author at: Department of Chemistry, Faculty of Science, Ain Shams University, Abassia, 11566, Cairo, Egypt.
Tel.: +966.595.5216274. Fax: +966.014.4251127. E-mail address: aymanaziz31@sci.asu.edu.eg (A.A.A. Aziz).

ARTICLE INFORMATION

ABSTRACT

Co(II), Ni(II), Cu(II) and Zn(II) metal complexes of a quadridentate Schiff base with a N_2S_2 donor set derived from condensation of benzene-1,2-dicarboxaldehyde(*o*-phthaldehyde) with 2-aminothiophenol were synthesized and characterized by elemental microanalyses, molar conductance, magnetic susceptibility measurements and spectroscopic techniques *viz*, FT-IR, ^{1}H NMR, EPR and UV-Vis. The spectral data showed that, the ligand acts as a tetradentate ligand and the bonding sites were deprotonated thiol-S groups and azomethine nitrogen atoms. The results have indicated that the complexes exhibited tetrahedral geometry arrangements except Cu(II) complex that exhibited square planar geometry. Preliminary antimicrobial screening shows the promising results against both bacterial and fungal strains. The interaction of the Schiff base ligand and its complexes with calf-thymus DNA (CT-DNA) has been monitored by UV-Vis, competitive fluorescence titration and hydrodynamic techniques (Viscosity measurements). The results have indicated that the ligand and its complexes bind to CT-DNA through intercalation mode. Moreover, investigations of antioxidative properties showed that all the compounds have strong radical scavenging properties. The data have shown that, among all compounds, Cu(II) complex has exhibited better biological activity than other complexes and the parent ligand.

1. Introduction

In recent years, there has been a rapid expansion in the development of metal complexes as extensive diagnostic agents/chemotherapeutic drugs [1]. In this regard, therapeutic agents that at pertain to less toxic and more effective metallic component are of particular interest and include a plethora of compounds: antitumor, antioxidant, antimicrobial and anti-flammatory agents [2]. Nitrogen-sulfur donor ligands have been of great interest to researchers [3]. The presence of nitrogen and/or sulfur atoms, provide these compounds with the ability to form metal complexes with heavy metal ions [4]. The fact that, the sulfur anion formed is more stabilized by negative charge distribution as reported [5]. Schiff bases containing N, S donor atoms and their metal complexes have received considerable attention [6-9]. Over the past few years, thio-Schiff bases and their metal complexes have received considerable attention in the field of coordination chemistry [10,11].

Thiosalen derivatives are Schiff base ligands where the sulfur atoms are substituted with oxygen atoms in salen ligands. The replacement of two phenoxide oxygen atoms in salen by two thiolate sulfur atoms lead to changes in the redox properties of the corresponding complexes. Since sulfur is a medium-strength soft base, it is often expected that coordination by sulfur will stabilize metals in low oxidation states, i.e., lead to a decrease in the potential of the complex based on the metal [12]. There have been numerous transition metal complexes containing salen and thiosalen, with two sulfur and two nitrogen donor atoms (N_2S_2 donor set) [12,13].

As a part of our investigation on Schiff bases and their metal complexes [14-20], we have recently reported the tetradentate Schiff base *N*,*N'*-*bis*-(2-aminothiophenol)benzene-1,2-dicarboxaldehyde (ATBD) and used it as a fluorescence sensor [19]. In continuation of our work, herein, we have synthesized Co(II), Ni(II), Cu(II) and Zn(II) complexes of the novel thiosalen Schiff base and the novel compounds were fully characterized by elemental analysis, FT-IR, ^{1}H NMR, EPR, electronic spectra, molar conductivity and magnetic suscep-tibility measurements. Moreover, the interaction with calf thymus DNA (CT-DNA), antioxidant scavenging and in vitro antimicrobial bacterial and antifungal activities of the novel compounds were investigated for applications in biotechno-logy and medicine.
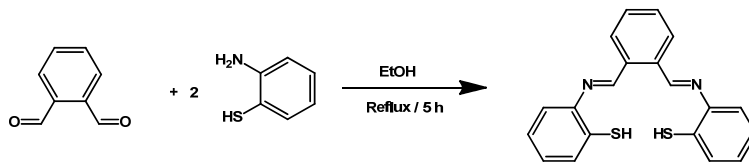
Scheme 1

2. Experimental

2.1. Materials

2-Aminothiohenol, *o*-phthaldehyde, $Co(OAc)_2.4H_2O$, $Ni(OAc)_2.4H_2O$, $Cu(OAc)_2.H_2O$ and $Zn(OAc)_2.2H_2O$ were supplied from Sigma-Aldrich. Calf thymus DNA (CT-DNA) and ethidium bromide (EB) were purchased from Sigma Chemicals Co. All solvents used were of analytical reagent grade and used without further purification.

2.2. Instrumentation

Microanalyses (C, H and N) were carried out on a Perkin-Elmer 240 elemental analyzer. The FT-IR spectra of the samples in 4000-400 cm^{-1} region were obtained in KBr discs on a Unicam-Mattson 1000 FT-IR. ^1H NMR spectra were recorded on a *Mercury 300 BB* spectrometer in DMSO-d_6 as a solvent. The molar conductivities of the complexes (1×10^{-3} M) in dimethylsulphoxide (DMSO) solution were measured at room temperature by using Jenway 4010 conductivity meter. Room temperature (298 K) magnetic susceptibilities were measured using a Sherwood Scientific balance using $Hg[Co(SCN)_4]$ as a calibrant. Diamagnetic corrections calculated from Pascal's constants [21] were used to obtain the molar paramagnetic susceptibilities. The X-band EPR spectrum of copper(II) complex was recorded at room temperature on Bruker EPR spectrometer at 9.706 GHz (X-band), using DPPH as the g-marker. The UV-Vis spectra were recorded on a Shimadzu UV 1800 Spectrophotometer, equipped with a PC, using UV Probe software, Ver. 2. Fluorescence spectra were recorded on a Jenway 6270 Fluorimeter at room temperature.

2.3. Syntheses

2.3.1. Synthesis of N,N'-bis-(2-aminothiophenol)benzene-1,2-dicarboxaldehyde (ATBD)

The Schiff base ligand *N,N'-bis*-(2-aminothiophenol) benzene-1,2-dicarboxaldehyde (ATBD) was synthesized by convenient method as described previously [22]. An ethanolic solution of 2-aminothiophenol (10 mmol) was mixed with an ethanolic solution of *o*-phthaldehyde (5 mmol), 2 drops of acetic acid and magnetically stirred in a round bottom flask. The reaction mixture was then refluxed for ~5 h at 60 °C in water bath and kept overnight. The resulting solution was then poured into crushed ice water. The orange precipitate formed was filtered and recrystallized from hot methanol and dried under vacuum in a desiccator over anhydrous $CaCl_2$ to get chromatographically (TLC) pure compound. Synthetic route of ATBD is shown in Scheme 1. ATBD ($C_{20}H_{16}N_2S_2$): Yield: 79%. FT-IR (KBr, ν, cm^{-1}): 2543 (m, S-H), 1612 (s, C=N), 798 (m, C-S). ^1H NMR (300 MHz, DMSO-d_6, δ, ppm): 3.46 (s, 2H, -SH), 8.26 (s, 2H, -CH=N), 6.74-7.57 (m, 12H, Ar-H). TOF-MS (*m/z*): 348 (M^+). Anal. calcd. for $C_{20}H_{16}N_2S_2$: C, 68.93; H, 4.64; N, 8.04, Found: C, 68.40; H, 4.39; N, 8.00%.

2.3.2. Synthesis of M(II) complexes (1-4)

M(II) complexes were prepared by using the following general procedure. Hot ethanolic solution (10 mL) of the Schiff base ABTD (1 mmol) and the metal acetate salt (1 mmol) in ethanol (10 mL) were mixed thoroughly and the resulting solution was stirred and heated on a hot plate at 80 °C for 4 h. The mixture was cooled to room temperature and poured into ice chilled ethanol, filtered, washed several times with hot petroleum ether (60-80 °C) and dried under vacuum in a desiccator over anhydrous $CaCl_2$.

Compound 1: Color: Green. Yield: 61%. FT-IR (KBr, ν, cm^{-1}): 1605 (s, C=N), 759 (m, C-S), 502 (w, Co-N). Anal. calcd. for $C_{20}H_{14}N_2S_2Co$: C, 59.25; H, 3.48; N, 6.91; Co, 14.53. Found: C, 57.80, H, 3.91, N, 6.52, Co, 14.37%. $\Lambda_m (\Omega^{-1}cm^2 mol^{-1})$: 3.9.

Compound 2: Color: Brown. Yield: 85%. FT-IR (KBr, ν, cm^{-1}): 1600 (s, C=N), 756 (m, C-S), 501 (w, Ni-N). Anal. calcd. for $C_{20}H_{14}N_2S_2Ni$: C, 59.28; H, 3.48; N, 6.91; Ni, 14.48. Found: C, 57.82, H, 3.92, N, 6.45, Ni, 14.39%. $\Lambda_m (\Omega^{-1}cm^2 mol^{-1})$: 9.5.

Compound 3: Color: Green. Yield: 82%. FT-IR (KBr, ν, cm^{-1}): 1606 (s, C=N), 793 (m, C-S), 501 (w, Cu-N). Anal. calcd. for $C_{20}H_{14}N_2S_2Cu$: C, 58.58; H, 3.44; N, 6.83; Cu, 15.49. Found: C, 57.71, H, 4.38, N, 6.12, Cu, 15.52%. $\Lambda_m (\Omega^{-1}cm^2 mol^{-1})$: 6.5.

Compound 4: Color: Brown. Yield: 77%. FT-IR (KBr, ν, cm^{-1}): 1608 (s, C=N), 794 (m, C-S), 503 (w, Zn-N). ^1H NMR (300 MHz, DMSO-d_6, δ, ppm): 8.26 (s, 2H, - CH=N), 6.99-7.78 (m, 12H, Ar-H). Anal. calcd. for $C_{20}H_{14}N_2S_2Zn$: C, 58.32; H, 3.42; N, 6.80; Zn, 15.76. Found: C, 55.51, H, 3.36, N, 6.69, Zn, 15.76%. $\Lambda_m(\Omega^{-1}cm^2 mol^{-1})$: 4.7.

2.4. Determination of the metal content of the complexes

2.4.1. Determination of copper (II)

An exact weight of 0.1 g of Cu(II) complex was dissolved in 40 mL conc. HNO_3. The solution was boiled to evaporate the acidic solution near dryness, add another amount of conc. HNO_3 and evaporated. This process was repeated several times then diluted by distilled water. The resultant solution was filtered to remove the precipitated ligand. Ammonium hydroxide solution was then added to neutralize the acidic solution and transferred to 50 mL measuring flask and completed with deionized water. 5 ml of the solution was then titrated with 0.01 M EDTA solution using murexide, as an indicator, to determine the end point, which was characterized by a colour change from yellow to orange [23].

2.4.2. Determination of nickel (II)

An exact weight of 0.1 g of Ni(II) complex was treated in a similar manner to the previous one. Ammonium hydroxide was also added until the nickel ions were converted to the nickel tetramine complex, which was judged by colour change from green to blue. Murexide was then added as an indicator and the solution was titrated with 0.01 M EDTA solution. The end point was detected by a colour change from orange to purple [24].

2.4.3. Determination of cobalt (II)

An exact weight of 0.1 g of Co(II) complex was treated in a similar manner to the previous one. To the cobalt (II) solution 0.1 M sodium acetate was added followed by murexide, as an indicator, ammonium hydroxide solution was added until the colour changes from orange to yellow. The solution was

titrated with 0.01 M EDTA solution. The end point was detected by a colour change from yellow to deep purple [24].

2.4.4. Determination of zinc (II)

An exact weight of 0.1 g of Zn(II) complex was dissolved in 40 mL conc. HNO₃. The acidic solution was treated in the same manner as the previous ones. In a conical flask, 5 mL of the solution were used for every titration. 5 mL of ammonia buffer solution (pH = 10) and 5 drops 0.1 % of Eriochrome Black T (EBT) were then added. The solution was titrated with 0.01 M EDTA solution. The end point was detected by a colour change from wine red to blue [25].

2.5. Antimicrobial screening

Antimicrobial activities of the synthesized compounds are investigated using agar well diffusion method [26]. Antibacterial activities are investigated against bacteria strains *Staphylococcus aureus*, *Pseudomonas aeruginosa*, *Escherichia coli*, and *Staphylococcus epidermidis*, whereas *Aspergillus niger*, *Aspergillus flavus*, *Culvularia lunata* and *Candida albicansare* used to test antifungal activities. The tested compounds were dissolved in DMSO (which has no inhibition activity), to get concentration of 1 mg/mL. The test was performed on potato dextrose agar (PDA) medium, which contains infusion of 200 g potatoes, 6 g dextrose and 15 g agar. Uniform size filter paper disks (three disks per compound) were impregnated by equal volume (10 μL) from the specific concentration of dissolved test compounds and carefully placed on incubated agar surface. After incubation for 36 h at 27 °C in the case of bacteria and 48 h at 24 °C in the case of fungi, inhibition of the organisms which evidenced by clear zone surround each disk was measured and used to calculate mean of inhibition zones. Streptomycin and Nystatin were used as standard reference in the case of bacteria and antifungal studies, respectively.

2.6. DNA-binding studies

Concentrated CT-DNA stock solution was prepared in 5 mM tris-Cl/50 mM NaCl in water at pH = 7.5 and stored at 4 °C and were used within four days. The concentration of DNA solution was determined by UV absorbance at 260 nm (ε = 6600 M⁻¹·cm⁻¹) [27]. Solution of CT-DNA in 5 mM tris-HCl/50 mM NaCl (pH = 7.5) gave a ratio of UV absorption at 260 nm and 280 nm A_{260}/A_{280} of ~1.8-1.9, indicating that the DNA was sufficiently free of protein [28]. In order to study the interaction of CT DNA with the compounds, they were initially dissolved in DMSO to obtain concentration of (1 mM). Mixing of such solutions with the aqueous buffer solutions used in the studies never exceeded 5% DMSO (*v:v*) in the final solution, which was needed due to low aqueous solubility of complexes. All studies were performed at room temperature.

The interaction of ATBD and its complexes **1-4** with CT-DNA has been studied with UV spectroscopy in order to investigate the possible binding modes to CT-DNA and to calculate the binding constants (K_b). The UV spectra of CT-DNA in the presence of each compound have been recorded for a constant CT-DNA concentration in diverse mixing ratios (r = [Compound]/[CT-DNA]). The binding constants of the compounds with CT-DNA, K_b, have been determined using the UV spectra of the complexes recorded for a constant concentration in the absence or presence of CT-DNA for diverse r values. Control experiments with 5% DMSO were performed and no changes in the spectra of CT-DNA were observed. The absorption titrations of the compounds were performed using a fixed concentration (25 μM) for compound to which increments of the CT-DNA stock solution were added. The interacted solutions were allowed to incubate for 5 min before the absorption spectra were recorded. The intrinsic

binding constants K_b, based on the absorption titration, were measured by monitoring the changes of absorption with increasing concentration of CT-DNA using the following Equation (1):

$$\frac{[CT-DNA]}{(\varepsilon_a - \varepsilon_f)} = \frac{[CT-DNA]}{(\varepsilon_b - \varepsilon_f)} + \frac{[CT-DNA]}{K_b(\varepsilon_b - \varepsilon_f)} \quad (1)$$

where [CT-DNA] is the concentration of DNA in base pairs, the apparent absorption coefficients ε_a, ε_f and ε_b correspond to A_{obs}/[Complex], extinction coefficient for the free complex and the extinction coefficient of the complex in the totally bound form, respectively. The data were fitted to Equation (1), with a slope equal to $1/(\varepsilon_a-\varepsilon_f)$ and y-intercept equal to $1/K_b(\varepsilon_b-\varepsilon_f)$ and K_b was obtained from the ratio of the slope to the intercept.

The competitive studies of each complex with EB have been investigated by fluorescence spectroscopy in order to examine whether the complex can displace EB from its EB-CTDNA complex. The EB-CT-DNA complex was prepared by adding 20 μM EB and 40 μM CT-DNA in buffer (150 mM NaCl and 15 mM trisodium citrate at pH = 7.0). The solutions were excited at 540 nm and fluorescence emission at 598 nm, were recorded. The samples were shaken and kept for 2-3 min for equilibrium and then the spectra were recorded. The intercalating effect of the complexes with the EB-CT-DNA complex was studied by adding a certain amount of a solution of the compound step by step into the solution of the EB-CT-DNA complex. The influence of the addition of each complex was monitored in the range of 560-700 nm. Commonly, fluorescence quenching can be described by the following Stern-Volmer (Equation 2) [29]:

$$\frac{I_o}{I} = 1 + K_{SV}[Q] \quad (2)$$

where I_0 and I are the steady-state fluorescence intensities in the absence and presence of quencher (Q), respectively. K_{sv} is the Stern-Volmer quenching constant, obtained from the slope of the plot of I_0/I versus [Q].

Hydrodynamic measurements, i.e. viscosity and sedimentation that are sensitive to length changes are regarded as the least ambiguous and most critical tests to a binding model in solution in the absence of crystallographic structural data [30]. Viscosity measurements were carried out using an Ostwald's capillary viscometer, immersed in a thermo stated water bath with the temperature setting at 25±0.1 °C. CT-DNA samples with an approximate average length of 200 base pairs were prepared by sonication in order to minimize complexities arising from DNA flexibility [31]. Titrations were performed for the studied compounds (0.0-5.0 μM), where each compound was introduced into a CT-DNA solution (0.30 mM) present in the viscometer. The flow times were measured with a digital stopwatch. Each sample was measured three times and an average flow time was recorded. The data were presented as $(\eta/\eta_o)^{1/3}$ *vs* [Compound]/[DNA] ratio [32], where η and η_o are the viscosity of DNA in the presence and absence of the studied compounds, respectively. The values of η and η_o were calculated by Equation (3):

$$\eta = \frac{t - t_0}{t_0} \quad (3)$$

where t is the observed flow time of CT-DNA containing solution and, t_o is the flow time of buffer alone. Relative viscosities for CT-DNA were calculated from the relation η/η_o.

2.7. Antioxidant assays

2.7.1. Superoxide radicals scavenging assay

The superoxide radicals ($O_2^{-\bullet}$) were generated in the test system using NBT/VitB₂/MET and determined spectro-

metrically by nitrobluetetrazolium photo reduction method [33-35]. The suppression of superoxide radicals was calculated by measuring the absorbance at 560 nm. ATBD and its metal complexes (5-25 μM) were added to a solution containing [NBT (65 μM), L-MET (13 mM), VitB$_2$ (1.5 μM), EDTA (0.1 mM)] and the resulting solution was made up to 2 mL with phosphate buffer (10 mM, pH = 7.0) in dark. The above mixture was illuminated with a white fluorescence lamp (15 W) for 15 min and the absorbance (A$_i$) was measured at 560 nm. The above mixture containing no investigated compounds was used as a control and its absorbance was taken as A$_0$. All the experiments were conducted in triplicate and data were expressed as the mean value. The suppression ratio for (O$_2^{-\bullet}$) was calculated by using following equation.

$$O_2^- \text{ Scavenging activity (\%)} = \frac{A_0 - A_i}{A_0} \times 100 \qquad (4)$$

The antioxidant activity was expressed as the 50% inhibitory concentration (IC$_{50}$). IC$_{50}$ values were calculated from regression lines where; x was the tested compound concentration in μM and *y* was percent inhibition of the tested compounds.

2.7.2. Hydroxy radical scavenging activity

The hydroxyl radicals (HO$^\bullet$) in aqueous media were generated through the Fenton system [35]. The solution of the tested compound was prepared with DMSO. An assay mixture (5 mL) contained the following reagents: safranin (11.4 μM), EDTA-Fe(II) (40 μM), H$_2$O$_2$ (0.6%), the tested compound (5-25 μM) and a phosphate buffer (67 mM, pH = 7.4). The assay mixtures were incubated at 45 °C for 50 min in a water-bath, and then the absorbance (A$_i$, A$_o$ and A$_c$) were measured at 520 nm. All the tests were run in triplicate and expressed as the mean value. The suppression ratio for (HO$^\cdot$) was calculated from the following expression:

$$HO^\cdot \text{Supression ratio (\%)} = \frac{A_i - A_o}{A_0 - A_c} \times 100 \qquad (5)$$

where A$_i$ = the absorbance in the presence of the tested compound; A$_o$ = the absorbance in the absence of the tested compound; A$_c$ = the absorbance in the absence of the tested compound, EDTA-Fe(II) and H$_2$O$_2$. The antioxidant activity was expressed as the 50% inhibitory concentration (IC$_{50}$). IC$_{50}$ values were calculated from regression lines where; x was the tested compound concentration in μM and *y* was percent inhibition of the tested compounds.

3. Results and discussion

The tetradentate Schiff base ligand, namely *N,N'-bis*-(2-aminothiophenol)benzene-1,2-dicarboxaldehyde (ATBD) was obtained by employing condensation reaction of *o*-phthaldehyde (1 mmol) with 2-aminothiophenol (2 mmol) under thermal condition. It is apparent that the ligand exhibit a considerable reactivity towards M(II) transition metals (M = Co(II), Ni(II), Cu(II) and Zn(II)), affording solid products which are fairly stable in air and moisture. The ligand and its complexes have been fully characterized by micro elemental analysis and different spectroscopic techniques. On the basis of elemental analyses, the Schiff base behaves as neutral tetradentate chelate with N$_2$S$_2$ donor atoms and the complexes are suggested to have 1:1 stoichiometry. The ligand and its complexes are freely soluble in dichloromethane (DCM), tetrahydrofuran (THF), dimethylformamide (DMF) and dimethyl sulfoxide (DMSO). The molar conductivities of complexes in DMSO (1×10^{-3} M solutions) indicate that all the metal complexes have conductivity values in accordance with non-electrolytes nature [36].

3.1. Infrared spectra

The mode of binding of the Schiff base (ATBD) to M(II) ions was elucidated by comparing the FT-IR spectra of the complexes with that of the free ligand. The FT-IR spectrum of parent Schiff base ligand show some main characteristic features, the first one is the appearance of the intense band at 1612 cm^{-1}, which is assigned to ν$_{(C=N)}$ (azomethine moiety), indicating the formation of the Schiff base [37], while the second feature is the appearance of medium intense band at 2543 cm^{-1}, which is attributed to ν$_{(S-H)}$. On comparison to the parent Schiff base ligand, upon complex formation, the ν$_{(C=N)}$ band is shifted towards lower frequencies in the spectra of metal complexes (1600-1608 cm^{-1}) indicating the involvement of the azomethine nitrogen in coordination with metal ion [38]. Furthermore, the disappearance of the ν$_{(S-H)}$ upon complexation was an indicative of deprotonation prior to coordination through the sulfur atom in all the complexes. Moreover the shift ν$_{(C-S)}$ band of ATBD at 798 cm^{-1} to 749-694 cm^{-1} in these complexes confirm the participation of thiol sulfur on chelation [39]. Conclusive evidence of the bonding is also shown by the observation that new bands in the spectra of all metal complexes appearing in the low frequency regions at 501-503 cm^{-1} which are characteristic to the ν$_{(M-N)}$ [10]. Thus, the FT-IR spectral data provide strong evidences for the complexation of the tetradentate Schiff bases with SNNS sequence.

3.2. ¹H NMR studies of ATBD and its Zn(II) complex

Evidence for the bonding mode of the ligand (ATBD) is provided also by the ¹H NMR spectra of the Schiff base and the diamagnetic Zn(II) complex which were recorded in DMSO-*d$_6$* at room temperature showed a sharp singlet signal at 8.26 ppm, assigned to the azomethine hydrogen atom. The shift of the imine carbon proton signal to downfield region in Zn(II) complex in comparison with that of the free ligand inferred coordination through the azomethine nitrogen atom of the ligand. The multiplet signals due to the aromatic protons, in ATBD in the range 6.74-7.57 ppm exhibited a shift in Zn(II) complex at 6.99-7.78 ppm, which may be attributed to the changes in the electronic environment around the protons attached to the group that contain the site of donation and involvement in complexation [40]. Furthermore, a comparison of ¹H NMR spectrum of diamagnetic Zn(II) complex showed that, the singlet signal at δ 3.46 ppm, assigned to thiol-SH protons was missed. The absence of -SH signal indicated the participation of thiol SH group in chelation with proton displacement and confirmed the bonding of sulfur to the metal ions (C-S-M).

3.3. Magnetic moments and electronic spectral analysis

Magnetic measurements and electronic spectra were recorded at room temperature in order to obtain information about the geometry of the complexes. Electronic spectra of ATBD and its complexes were recorded in DMSO (1×10^{-5} M) in the range 200-800 nm. The UV-visible spectrum of free ATBD exhibit two intense bands at 289 and 350 nm, assigned to intraligand (IL) π-π* and n-π* of benzene and non-bonding electrons present on the nitrogen of the azomethine moiety. In the complexes spectra, the π-π* and n-π* transitions experiences some shift due to coordination of imino nitrogen atom moiety. Co(II) complex **1** showed a magnetic moment of 4.62 B.M., suggesting four-tetrahedral geometry. The electronic spectra of the Co(II) complex **1** showed an absorption band at 624 nm assignable to $^4A_2(F) \rightarrow {}^4T_1(P)$, which is characteristic value for the tetrahedral Co(II) complex. The observed magnetic moment of Ni(II) complex was 3.23 B.M. which indicated the non-coupled mononuclear complex of *d^8* system with s = 1 spin state of tetrahedral geometry [41,42].

Table 1. Magnetic moment values and electronic absorption spectral data of Schiff base (ATBD) its complexes **1**-**4**.

Compound	μ_{eff} (B.M)	λ_{max} (nm)	Assignments	Geometry
ATBD	-	289	$\pi \rightarrow \pi^*$	-
		350	$n \rightarrow \pi^*$	
[$C_{20}H_{14}N_2S_2Co$] (**1**)	4.62	290	$\pi \rightarrow \pi^*$	Tetrahedral
		345	$n \rightarrow \pi^*$	
		624	$^4A_2(F) \rightarrow {}^4T_1(P)$	
[$C_{20}H_{14}N_2S_2Ni$] (**2**)	3.23	286	$\pi \rightarrow \pi^*$	Tetrahedral
		355	$n \rightarrow \pi^*$	
		532	$^3T_1(F) \rightarrow {}^3T_1(P)$	
		692	$^3T_1(F) \rightarrow {}^3A_2(F)$	
[$C_{20}H_{14}N_2S_2Cu$] (**3**)	1.73	279	$\pi \rightarrow \pi^*$	Square planar
		344	$n \rightarrow \pi^*$	
		457	$^2B_{1g} \rightarrow {}^2E_g$	
		647	$^2B_{1g} \rightarrow {}^2A_{1g}$	
[$C_{20}H_{14}N_2S_2Zn$] (**4**)	-	280	$\pi \rightarrow \pi^*$	Tetrahedral
		344	$n \rightarrow \pi^*$	
		402	MLCT	

M = Co(II), Ni(II) and Zn(II) M = Cu(II)
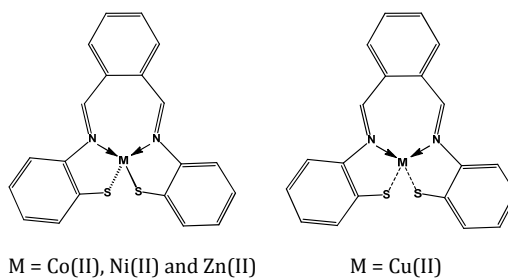
Scheme 2

The electronic absorption of the Ni(II) complex **2** showed two bands in the visible region at 692 and 532 nm which are assigned to $^3T_1(F) \rightarrow {}^3A_2(F)$ (ν_2) and $^3T_1(F) \rightarrow {}^3T_1(P)$ (ν_3) transitions, respectively suggesting a tetrahedral geometry around Ni(II) ion. On the other hand, the observed magnetic moments (μ_{eff}) of Cu(II) complex **3** at room temperature was 1.73 B.M., which was consistent with presence of a single unpaired electron [43] and suggesting that the square-planar geometry [44]. The electronic spectrum of the Cu(II)complex **3** showed two bands at about 647 and 457 nm which could be assigned to $^2B_{1g} \rightarrow {}^2A_{1g}$ and $^2B_{1g} \rightarrow {}^2E_g$ transitions, respectively [44], indicating the square planar geometry for Cu(II) complex. Finally, the electronic spectrum of the Zn(II) complex **4** showed one high-intensity band at 402 nm, which was assigned to metal-to-ligand charge transfer [45]. It is known that the Zn(II) complex is diamagnetic as expected for a d^{10} configuration and on the basis of analytical, conductance and infrared spectral data, a tetrahedral geometry is proposed for the Zn(II) complex. The electronic spectral data of ATBD and its complexes along with magnetic moment values with tentative assignments are summarized in Table 1. Based on the above spectral data expected structures for the prepared complexes were presented in Scheme 2.

3.4. EPR spectral studies

EPR studies of paramagnetic transition metal complexes give information about the distribution of the unpaired electrons and hence about the nature of the bonding between the metal ion and its ligand [46]. The X-band EPR spectrum of Cu(II) complex was recorded in the solid state at room temperature (Figure 1). The Cu(II) complex exhibit typical axial behavior with slightly different $g_{||}$ and $g_\perp$ values. For Cu(II) complex at room temperature, $g_{||}$= 2.09076, $g_\perp$ = 2.06345 and g_{av}= 2.08165. The $g_{||} > g_\perp > 2.0023$ indicates that the unpaired electron is present in the d_{x2-y2} ground state in a square planar geometry [47]. Moreover, $g_{||} < 2.3$ value suggests covalent character of the metal-ligand bond [48]. This is

further supported by calculating the axial symmetry parameter (G), which is a measure of exchange coupling interaction between two Cu(II) ions using Kneubuhl's method [49], G = ($g_{||}$-2.0023)/($g_\perp$-2.0023). According to Hathaway [50], if the G value was > 4, the exchange interaction is negligible, while a value of < 4 indicated a considerable exchange interaction in the complex. The axial symmetry parameter (G) of Cu(II) complex was 1.4466 indicating considerable exchange interaction in the solid complexes [51]. Thus, the EPR study of Cu(II) complex has provided supportive evidence to the conclusion obtained on the basis of electronic spectrum and magnetic moment value.
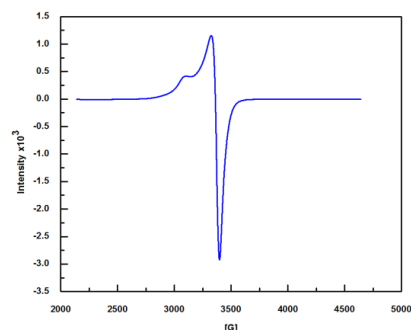
Figure 1. EPR spectrum of Cu(II) complex at room temperature.

3.5. Bioactivity evaluation

Thiol containing compounds play an important role in protecting biological systems against oxidative injury. There is also increasing evidence for thiol involvement in metabolic regulation, signal transduction and regulation of gene expression [52]. Physiological thiols vary substantially in their reactivity, and on this basis, thiol groups would be preferred cellular targets for various oxidants [53].

3.5.1. Antimicrobial activity

The Schiff base complexes have provoked wide interest because they possess a diverse spectrum of biological and pharmaceutical activities. Consequently, the antibacterial activity of the Schiff base ligand and its metal complexes were tested against bacteria because bacteria can achieve resistance to antibiotics through biochemical and morphological modifications [54]. The bacteria strains used in the present investigation included *S. aureus*, *P. aeruginosa*, *E. coli*, *S. epidermidis*. Furthermore, the synthesized Schiff base and its metal complexes were screened in vitro in order to find out the antifungal activity against the fungi strains *A. niger*, *A. flavus*, *C. lunata* and, *C. albicans*. The results of the antibacterial and antifungal activities are graphically represented in Figure 2. The results of antibacterial and antifungal reveals that the metal complexes are toxic than the free ligand against the same organisms. It is suggested that the complexes having antibacterial and antifungal activities through inhibition multiplication process of the microbe by blocking their active sites [55]. The mechanism of toxic activity of the complexes relative to the ligand can be ascribed to the increase in the lipophilic nature of the complexes arising from chelation. Chelation reduces the polarity of the metal atom mainly because of partial sharing of its positive charge with the donor groups and possible π-electron delocalization within the whole chelate ring. Moreover, the chelation also increases the lipophilic nature of the metal atom, which subsequently favors the permeation through the lipid layer of cell membrane. The mode of action of complexes involves the formation of hydrogen bonds with the imino group by the active sites leading to interference with the cell wall synthesis. This hydrogen bond formation damages the cytoplasmic membrane and the cell permeability may also be altered leading to cell death [56].

3.5.2. DNA binding studies

It is a well-known fact that CT-DNA is the primary pharmacological target of many antitumor compounds, and hence the interaction between CT-DNA and metal complexes is of paramount importance in understanding the mechanism. Thus, the mode and propensity for binding of the complex to CT-DNA were studied with the aid of different techniques. Monitoring the changes in the absorption spectra of ATBD and its complexes **1**-**4** upon addition of increasing amounts of CT-DNA is one of the most widely used methods for determining the overall binding constants. Upon the addition of CT-DNA, hyperchromism and hypochromism in the absorbencies of the *d-d* transition absorption bands of the complexes were observed [57]. The extent of the hypochromism commonly parallels the intercalative binding strength [58]. The hypochromicity, characteristic of intercalation has been usually attributed to the interaction between the electronic states of the compound chromophores and those of the CT-DNA bases [59], while the hyperchromicity (red shift) has been associated with the decrease in the energy gap between the highest and the lowest molecular orbitals (HOMO and LUMO) after binding of the complex to CT-DNA [60].

Absorption titration experiments were performed by maintaining the studied compounds concentration as constant at 25 μM while varying the concentration of the DNA within 0-50 μM (Figure 3). As shown in Figure 3, it was obviously that, a significant hypochromism with a red shift of 3, 8, 5, 14 and 4 nm for ATBD and its complexes **1**-**4**, respectively, suggesting strong binding to CT-DNA in an intercalative mode. In order to compare quantitatively, the binding strength with CT-DNA, the intrinsic binding constants K_b of the reported compounds (Figure 3 insets) were determined. The K_b values were found to be $(5.82 \pm 0.15) \times 10^4$ M^{-1}, $(8.78 \pm 0.35) \times 10^5$ M^{-1}, $(2.51 \pm 0.28) \times 10^5$ M^{-1}, $(4.17 \pm 0.13) \times 10^6$ M^{-1} and $(1.55 \pm 0.10) \times 10^5$ M^{-1} for

ATBD and its complexes **1**-**4**, respectively. These values indicated that, the order of binding affinity is 3 > 1 > 2 > 4 > ATBD. The K_b values of complexes are higher than that of the classical intercalator EB ($K_b = (1.23 \pm 0.07) \times 10^5$ M^{-1}) [61], which may be a first evidence of the ability of the compounds to displace EB in the case of intercalation except ATBD Schiff base ligand. An explanation for higher K_b value of Cu(II) complex is apparently that copper is 'borderline' metal which show high affinity for both nucleobases and phosphate [62].
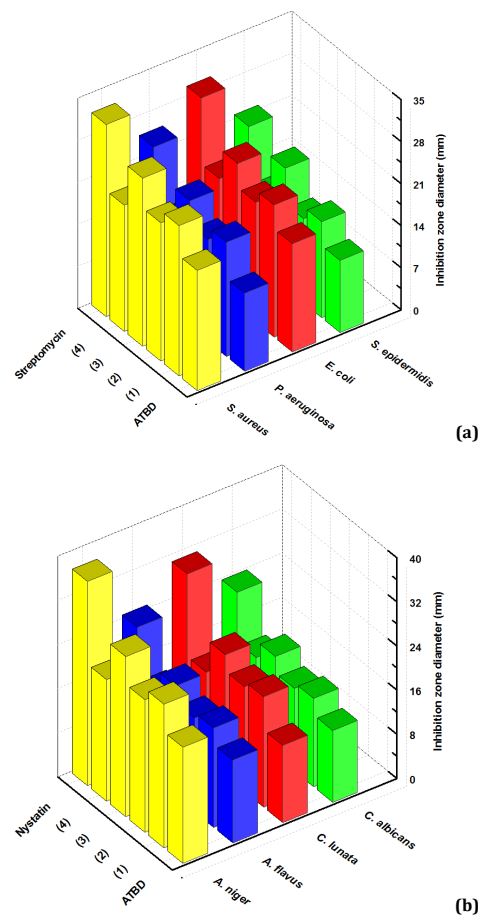

Figure 2. Biological diagram of Schiff base (ATBD) and its complexes **1**-**4** against (a) bacteria strains and (b) fungi strains.

Ethidium bromide (EB = 3,8-diamino-5-ethyl-6-phenyl phenanthridinium bromide) emits intense fluorescence in the presence of CT-DNA as a result of strong intercalation of the planar EB phenanthridine ring between adjacent base pairs on the double helix; therefore, EB is considered a typical indicator of intercalation [63]. The changes observed in the fluorescence emission spectra of a solution containing EB bound to CT-DNA may be used to study the interaction between CT-DNA and other compounds, such as metal complexes, since the addition of a compound, capable to intercalate to CT-DNA equally or more strongly than EB, could result in a quenching of the EB-CT-DNA fluorescence emission [64]. Steady-state competitive binding experiments using complexes **1**-**4** were undertaken to get further proof for the binding of the complexes to DNA. The displacement technique is based on the decrease of EB fluorescence resulting from the competitive displacement of EB from a CT-DNA groove by a compound that competes for the same site.

The fluorescence quenching curves of EB bound to CT-DNA by the reported complexes is shown in Figure 4.
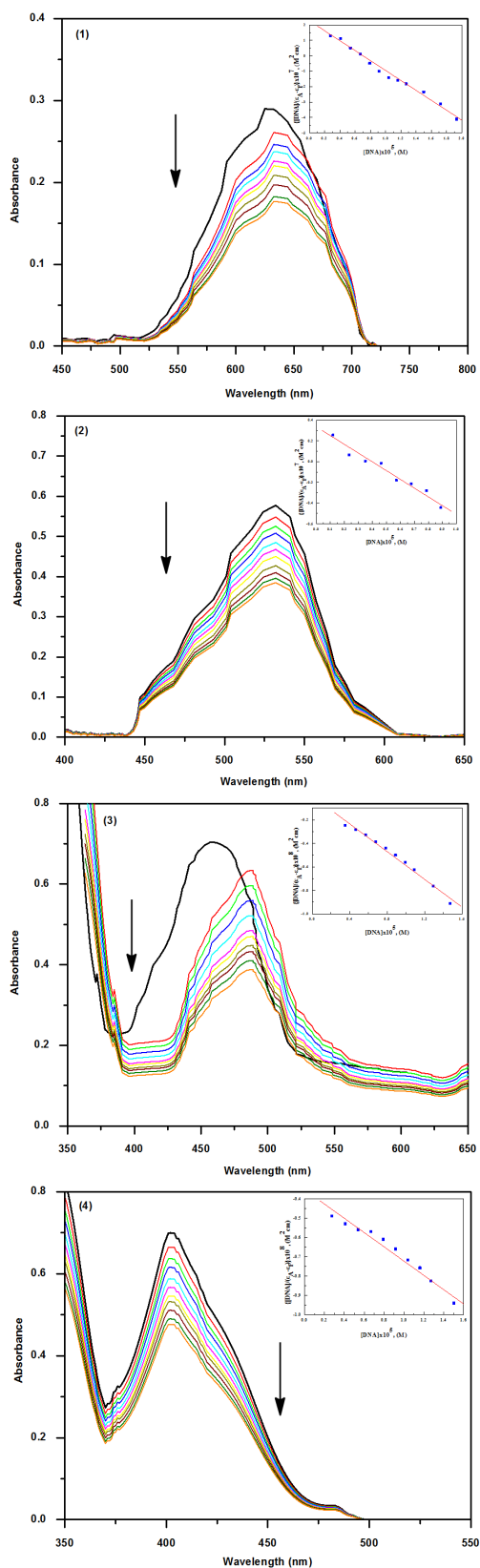
Figure 3. Absorption spectra of M(II) complexes **1-4** (25 μM) in the absence and presence of increasing amounts of CT-DNA. Conditions: [Complex = 25 μM, [CT-DNA] = 0-50 μM. Arrow (↓) shows the absorbance changes upon increasing CT-DNA concentration. Inset: linear plot for the calculation of the intrinsic CT-DNA binding constant (K_b).
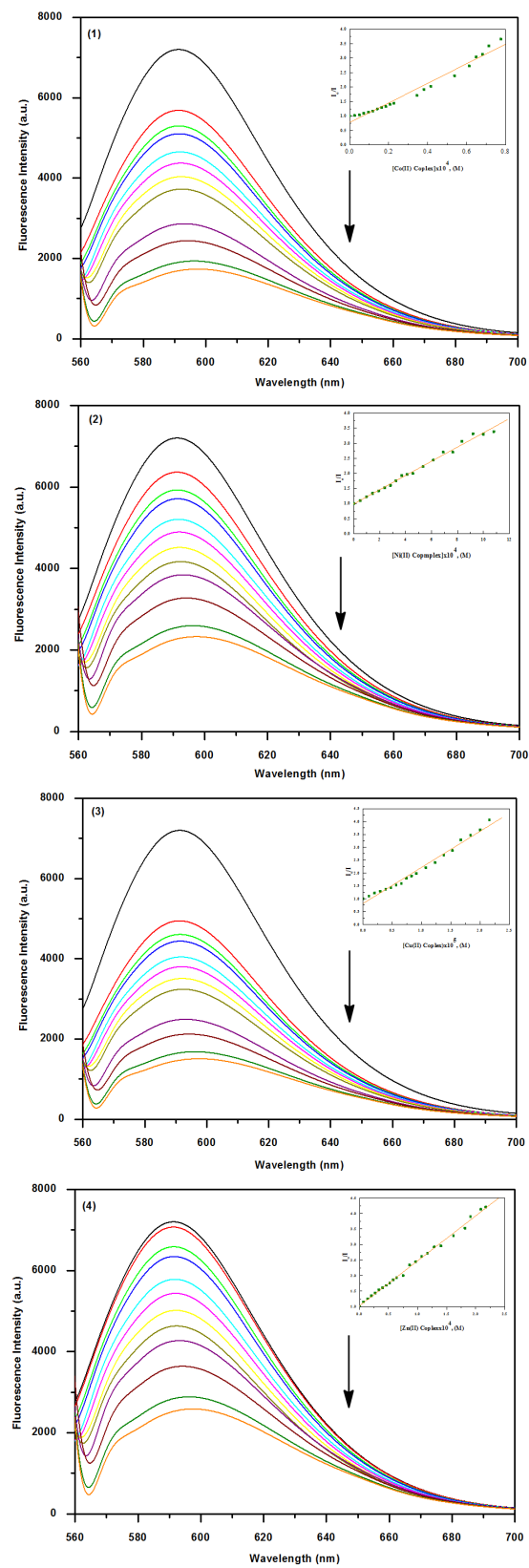
Figure 4. Emission spectra of EB-CT-DNA system in absence and presence of different M(II) complexes **1-4**. An arrow indicates the emission intensity changes upon increasing complex concentrations. Inset: Stern-Volmer quenching curves.

As it is shown, the addition of complexes to CT-DNA pretreated with EB causes appreciable reduction in the emission intensity, indicating that the EB-CT-DNA fluorophore is partially replaced by the reported complexes. Furthermore, the Stern-Volmer plots of EB-CT-DNA (Figure 4 insets) illustrate that the quenching of EB bound to CT-DNA by the complexes is in good agreement (R = 0.99) with the linear Stern-Volmer equation (Equation 2) [65,66], which also indicates that the complexes bind to CT-DNA. The K_{SV} values (Stern-Volmer constant) obtained by Stern-Volmer plots of DNA-EB are $(3.39\pm0.13) \times 10^4$ M^{-1}, $(2.36\pm0.05) \times 10^4$ M^{-1}, $(1.40\pm0.05)\times10^5$ M^{-1} and $(1.45\pm0.02)\times10^4$ M^{-1}, respectively, which suggests that the interaction of complexes with CT-DNA is a moderate intercalative mode following the order 3 > 1 > 2 > 4.

To further clarify the interactions between the compounds and CT-DNA, viscosity measurements were carried out. Viscosity measurements that are sensitive to length change are regarded as the least ambiguous and the most critical tests of binding model in solutions in the absence of crystallographic structural data. The viscometric measurement is also an important tool to find the nature of binding of metal complexes to the CT-DNA. A classical intercalation model results in the lengthening of the CT-DNA helix as the base pairs is separated to accommodate the binding molecule, leading to an increase in the CT-DNA viscosity. However, a partial and non-classical intercalation may bend (or kink) CT-DNA helix, resulting in the decrease of its effective length and concomitantly its viscosity [67]. The relative specific viscosity of CT-DNA is determined by varying the concentration of the added compounds. The plots of $(\eta/\eta_0)^{1/3}$ versus R, (where R = [Compound]/[CT-DNA] (Figure 5) give a measure of the viscosity changes. As shown in Figure.5, the relative viscosity of CT-DNA double helix exhibited an increase as a result of intercalation, suggesting primarily groove binding nature of the complexes. Groove (or) surface binding can cause an increase in the effective length of DNA leading to a minor increase in the effective length of CT-DNA solution [68].
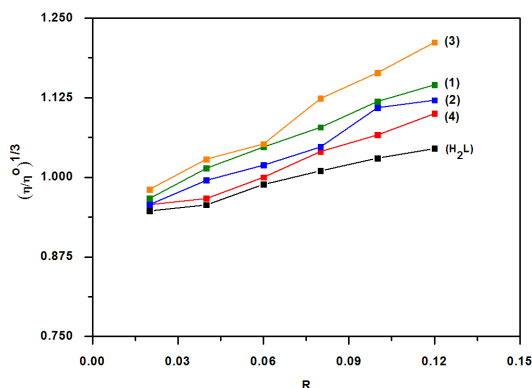

Figure 5. Effect of increasing amounts of ATBD and its M(II) complexes **1-4** on the on the relative viscosities of CT-DNA at room temperature (R = [Complex]/[CT-DNA]).

3.5.3. Evaluation of radical scavenging ability

Schiff base metal complexes are known to show various biological activities including biocidal and antioxidant activities [69,70]. In view of this and significant DNA binding affinity shown by the reported Schiff base complexes used in the present study, it is considered worthwhile to study the antioxidant properties of these compounds. Reactive oxygen species (ROS) e.g. superoxide (O_2^{-}•) and hydroxyl (HO•) radical are responsible for the disintegration of cell membrane and damage to protein and DNA structures. As shown in Figure 6a, increasing concentration (5-25 µM) of all the complexes

showed increasing inhibitory activities against ROS. Among the studied complexes, Cu(II) complex and Co(II) complexes showed highest superoxide scavenging ability of 97% and 80% respectively, in contrast to 70% and 66 % inhibition obtained in case of Ni(II) and Zn(II) complexes at a concentration of 25 µM. Moreover, the ATBD Schiff base and its metal complexes at the same concentration (5-25 µM) were also screened for the HO• radical scavenging activity (Figure 6b). It is evident from the results that both Cu(II) and Co(II) complexes are better scavenging agents (87% and 74%) than Ni(II) and Zn(II) complexes, which showed 53 and 50% scavenging activities respectively at a concentration of 25 µM. This trend can be correlated with the fact that Cu(II) and Co(II) complexes have shown stronger CT-DNA binding ability than Ni(II) and Zn(II) complexes.
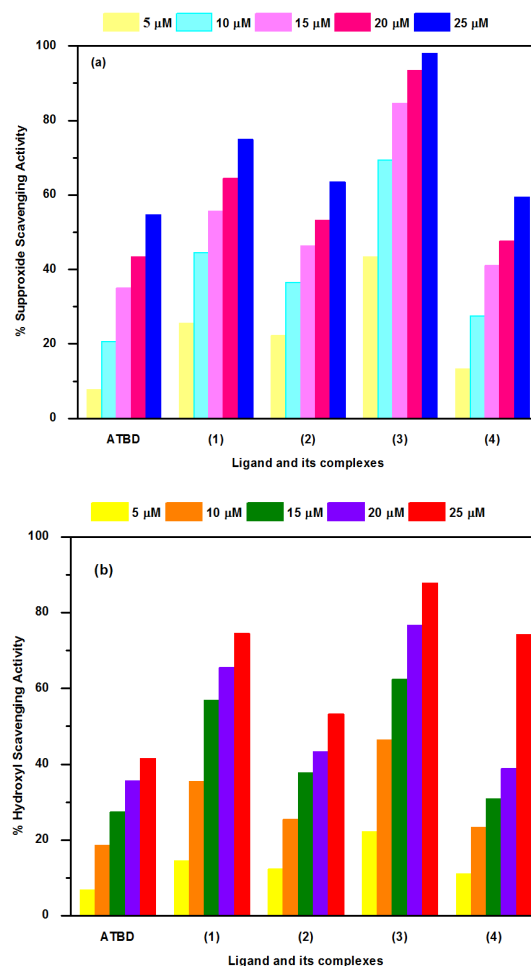
Figure 6. Scavenging effect of ATBD Schiff base and its complexes **1-4** on (a) superoxide radical and (b) hydroxyl radical.

The scavenging activities of ATBD and its complexes **1-4** against both superoxide and hydroxyl radicals are listed in Table 2 and 3. The IC$_{50}$ values indicated that the reported compounds showed antioxidant activity in the order of 3 > 1 > 2 > 4 > ATBD in all the experiments (Figure 7).

4. Conclusion

In the present work, four mononuclear M(II) complexes (M = Co, Ni, Cu and Zn) of potentially tetradentate N_2S_2 Schiff base namely: *N,N'-bis*-(2-aminothiophenol)benzene-1,2-dicarbox aldehyde have been synthesized and characterized by physicochemical and spectroscopic methods.
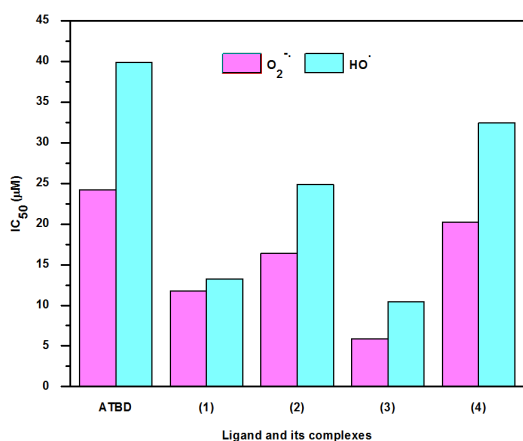
Table 2. The scavenging activities of Schiff base (ATBD) and its complexes **1-4** against superoxide radical.

Compound	% Superoxide scavenging activity ($O_2^{-\bullet}$)					Equation	IC_{50} (µM)	r^2
	5 µM	10 µM	15 µM	20 µM	25 µM			
ATBD	7.64	20.58	34.99	43.33	54.66	$y = 66.13x - 41.48$	24.17	0.969
$[C_{20}H_{14}N_2S_2Co]$ (**1**)	25.55	44.44	55.65	64.44	74.89	$y = 68.55x - 23.42$	11.77	0.991
$[C_{20}H_{14}N_2S_2Ni]$ (**2**)	22.22	36.55	46.33	53.22	63.54	$y = 56.79x - 18.94$	16.36	0.981
$[C_{20}H_{14}N_2S_2Cu]$ (**3**)	43.33	69.44	84.66	93.44	98.01	$y = 79.90x - 11.3$	5.85	0.993
$[C_{20}H_{14}N_2S_2Zn]$ (**4**)	13.33	27.55	40.99	47.66	59.33	$y = 63.93x - 33.49$	20.22	0.976

Table 3. The scavenging activities of Schiff base (ATBD) and its complexes **1-4** against hydroxyl radical.

Compound	% Hydroxyl scavenging activity ($HO^\bullet$)					Equation	IC_{50} (µM)	r^2
	5 µM	10 µM	15 µM	20 µM	25 µM			
ATBD	6.77	18.55	27.33	35.55	41.44	$y = 49.50x - 29.25$	39.90	0.986
$[C_{20}H_{14}N_2S_2Co]$ (**1**)	14.43	35.41	56.88	65.54	74.43	$y = 87.62x - 48.34$	13.25	0.990
$[C_{20}H_{14}N_2S_2Ni]$ (**2**)	12.32	25.42	37.64	43.29	53.28	$y = 56.21x - 28.48$	24.89	0.985
$[C_{20}H_{14}N_2S_2Cu]$ (**3**)	22.22	46.44	62.39	76.59	87.69	$y = 93.01x - 44.63$	10.41	0.993
$[C_{20}H_{14}N_2S_2Zn]$ (**4**)	11.11	23.31	30.86	38.88	74.11	$y = 49.8x - 25.26$	32.45	0.976

Figure 7. Radical scavenging activity of Schiff base (ATBD) and its metal complexes **1-4**.

The spectral data showed that the Schiff base act as a tetradentate ligand by bonding to the metal ion through the deprotonated thiol-S groups and azomethine nitrogen atoms. The binding properties of the complexes with CT-DNA were examined by various techniques, and the results suggest that the investigated compounds bind to CT-DNA via intercalation mode. Moreover, the binding constants showed that the complexes have a higher binding affinity than their parent ligand. In view of significant DNA binding affinity observed, the antioxidant properties of these compounds were considered worthwhile to study. The results show that, the complexes show stronger antioxidant activities than the ligand alone with highest activity in case of Cu(II) complex. In view of the data obtained, the novel complexes would be helpful to understand the interaction mechanism of the complexes with CT-DNA and are promising therapeutic drug candidates.

Acknowledgements

References

[1]. Gielen, M.; Tiekink, E. R. T. Metallotherapeutic Drugs and Metal-Based Diagnostic Agents, the Use of Metals in Medicine, Wiley, Chichester, 2005.
[2]. Marzano, C.; Pellei, M.; Tisato, F.; Santini, C. *Med. Chem.* **2009**, *9,* 185-211.
[3]. Arora, M.; Saravanan, J.; Mohan, S.; Bhattacharjee, S. *Int. J. Pharm. Pharm. Sci.* **2013**, *5*, 315-319.
[4]. Jozlowski, C. A.; Ulewicz, M.; Walkowiak, W.; Girek, T.; Tablonska, J. *Miner. Eng.* **2002**, *15*, 677-682.
[5]. Pandy, J. K.; Sengupta, S. K.; Pandey, O. P. *J. Indian Chem. Soc.* **2006**, *83*, 107-109.
[6]. Rai, B. K.; Choudhary, P.; Rana, S.; Sahi, P. *Orient. J. Chem.* **2007**, *23*, 271-275.
[7]. Rodriguez-Argueelles, M. C.; Touron-Touceda, P.; Cao, R.; Garcia-Deibe, A. M.; Pelagatti, P.; Pelizzi, C.; Zani, F. *J. Inorg. Biochem.* **2009**, *103*, 35-42.
[8]. Chan, J.; Thompson, A. L; Jones, M. W.; Peach, J. M. *Inorg. Chim. Acta* **2010**, *363*, 1140-1149.
[9]. Bal, T.; Atasever, B.; Solakoğlu, Z.; Erdem-Kuruca, S.; Ulküseven, B. *Eur. J. Med. Chem.* **2007**, *42*, 161-167.
[10]. Huo, J.; Liu, K.; Zhao, X.; Zhang, X.; Wang, Y. *Spectrochim. Acta* A **2014**, *117*, 789-792.
[11]. Pallikkavil, R.; Ummathur, M. B.; Krishnankutty, K. *Arch. Appl. Sci. Res.* **2012**, *4*, 2223-2227.
[12]. Butin, K. P.; Moiseeva, A. A.; Beloglazkina, E. K.; Chudinov, Y. B.; Chizhevskii, A. A.; Mironov, A. V.; Trasevich, B. N.; Lalov, A. V.; Zyk, N. V. *Russ. Chem. Bull. Int. Ed.* **2005**, *54*, 173-188.
[13]. Taylor, M. K.; Trotter, K. D.; Reglinski, J.; Berlouis, L. E. A.; Kennedy, A. R.; Spickett, C. M.; Sowden, R. J. *Inorg. Chim. Acta* **2008**, *361*, 2851-2862.
[14]. Abdel Aziz, A. A. *Synth. React. Inorg. Met. Org. Chem.* **2011**, *41*, 384-393.
[15]. Bahaffi, S. O.; Abdel Aziz, A. A.; El-Naggar M. M. *J. Mol. Struct.* **2012**, *1020*, 188-196.
[16]. Abdel Aziz, A. A.; Badr, I. H. A.; El-Sayed, I. S. A. *Spectrochim. Acta A* **2012**, *97*, 388-396.
[17]. Abdel Aziz, A. A.; Salem, A. M.; Sayed, M. A.; Aboaly, M. M. *J. Mol. Struct.* **2012**, *1010*, 130-1138.
[18]. Abdel Aziz, A. A. *J. Lumin.* **2013**, *143*, 663-669.
[19]. Abdel Aziz, A. A. *Synth. React. Inorg. Met. Org. Chem.* **2014**, *44*, 1137-1153.
[20]. Abdel Aziz, A. A.; Seda, S. H. *Sens. Actuat. B.* **2014**, *197*, 155-163.
[21]. Earnshaw, A. Introduction to Magnetochemistry, Academic Press: London, 1968.
[22]. Abdel Aziz, A. A.; Mohammed, S. F.; El Gamel, M. M. *J. Fluo.* **2014**, *24*, 859-874.
[23]. Rishi, A. K.; Garg, B. S.; Singh, R. P. *Fresen. J. Anal. Chem.* **1972**, *259*, 288.
[24]. Vogel, A. I. Text Book of Quantitative Chemical Analysis, 5th edition, Longmans, London, 1998.
[25]. Macarovici, C. G. Inorganic Quantitative Chemical Analysis; Editura Academiei R. S. R., Bucureti, 1979.
[26]. Bauer, A. W.; Kirby, W. W. M.; Sherris, J. C.; Turck, M. *Am. J. Clin. Pathol.* **1966**, *45*, 493-496.
[27]. Marmur, J. *J. Mol. Biol.* **1961**, *3*, 208-218.
[28]. Reichmann, M. E.; Rice, C. A.; Thomos, C. A.; Doty, P. *J. Am Chem. Soc.* **1954**, *76*, 3047-3053.
[29]. Lakowicz, J. R. Principles of Fluorescence Spectroscopy, 3rd edition, Springer Science, Business Media: New York, 2006.
[30]. Chaires, J. B.; Dattagupta, N.; Crothers, D. M. *Biochemistry* **1982**, *21*, 3933-3940.
[31]. Satyanaryana, S.; Dabrowial, J. C.; Chaires, J. B. *Biochemistry* **1993**, *32*, 2573-2584.
[32]. Eriksson, M.; Leijon, M.; Hiort, C.; Norden, B.; Gradsland, A. *Biochemistry* **1994**, *33*, 5031-5040.
[33]. Khan, N. H.; Pandya, N.; Kumar, M.; Bera, P. K.; Kureshy, R. I.; Abdi, S. H. R.; Bajaj, H. C. . *Org. Biomol. Chem.* **2010**, *19*, 4297-4307.
[34]. Suksrichavalit, T.; Prachayasittikul, S.; Nantasenamat, C.; Na-Ayudhya, C. I.; Prachayasittikul, V. *Eur. J. Med. Chem.* **2009**, *44*, 3259-3265.
[35]. Dreher, D.; Junod, A. F. *Eur. J. Cancer* **1996**, *32*, 30-38.

[36]. Dean, J. A. Lange's Hand Book of Chemistry, 4th edition, McGraw-Hill, New York, 1992.
[37]. Emara, A. A. A.; El-Sayed, B. A.; Ahmed, A. E. *Spectrochim. Acta A* **2008**, *69*, 757-769.
[38]. Mayadevi, S.; Prasad, P. G.; Yusuff, K. K. M. *Synth. React. Inorg. Met. - Org. Nano-Met. Chem.* **2003**, *33*, 481-496.
[39]. Durmus, S.; Atahan, A.; Zengin, M. *Spectrochim. Acta A* **2011**, *84*, 1-5.
[40]. Naeimi, H.; Safari, J.; Heidarnezhad, A. *Dyes Pigm.* **2007**, *73*, 251-253.
[41]. Cotton, F. A.; Wilkinson, G. Advanced Inorganic Chemistry, 5th edition, Wiley, New York, 1988.
[42]. Konstantinovic, S. S.; Radovanovic, B. C.; Krkljes, A. *J. Therm. Anal. Calorim.* **2007**, *90*, 525-531.
[43]. Cotton, F. A.; Wilkinson, C. W. Advanced Inorganic Chemistry, 3rd edition, Interscience Publisher, New York, 1972.
[44]. Lever, A. B. P. Inorganic Electronic Spectroscopy, 2nd edition, Elsevier, Amsterdam, 1984.
[45]. Raman, N.; Pothiraj, K.; Baskaran, T. *J. Mol. Struct.* **2011**, *1000*, 135-144.
[46]. Dhanaraj, C. J.; Johnson, J. *Spectrochim. Acta A* **2014**, *118*, 624-631.
[47]. Abd-Elzaher, M. M.; Moustafa, S. A.; Mousa, H. A.; Labib, A. A. *Monatsh Chem.* **2012**, *143*, 909-915.
[48]. Geeta, B.; Shravankumar, K.; Reddy, P. M.; Ravikrishna, E.; Sarangapani, M.; Reddy, K. K.; Ravinder, V. *Spectrochim. Acta A* **2010**, *77*, 911-915.
[49]. Kneubühl, F. K. *J. Chem. Phys.* **1960**, *33*, 1074-1078.
[50]. Hathaway, B. J.; Billing, D. E. *Coord. Chem. Rev.* **1970**, *5*, 143-207.
[51]. Singh, K.; Kumar, Y.; Puri, P.; Sharma, C.; Aneja, K. R. *Int. J. Inorg. Chem.* **2012**, *2012*, 1-9.
[52]. Kettle, A. J.; Winterbourn, C. C. *Redox. Rep.* **1997**, *3*, 3-15.
[53]. Hassan, W.; Rocha, J. B. T. *Molecules* **2012**, *17*, 12287-12296.
[54]. Raman, N.; Sobha, S. *Spectrochim. Acta A* **2012**, *85*, 223-234.
[55]. Ramesh, R.; Maheswaran, S. *J. Inorg. Biochem.* **2003**, *96*, 457-462.
[56]. Tweedy, B. G. *Phytopathology* **1964**, *55*, 910-914.
[57]. Vyas, K. M.; Joshi, R. G.; Jadeja, R. N.; Prabha C. R.; Gupta, V. K. *Spectrochim. Acta A* **2011**, *84*, 256-268.
[58]. Chow, C. S.; Barton, J. K. *Methods Enzymo.* **1992**, *212,* 219-242.
[59]. Wang, B. D.; Yang, Z. Y.; Crewdson, P.; Wang, D. Q. *J. Inorg. Biochem.* **2007**, *101*, 1492-1504.
[60]. Tan, J. H.; Lu, Y.; Huang, Z. S.; Gu, L. Q.; Wu, J. Y. *J. Inorg. Chem.* **2007**, *42*, 1169-1175.
[61]. Lakowicz, J. R.; Weber, G. *Biochemistry* **1973**, *12*, 4161-14170.
[62]. Larson, C. J.; Verdine, G. L. in: Hecht, S. M. (Ed.), Bioorganic Chemistry Nucleic Acids, Oxford University Press, New York, 1996.
[63]. Dhar, S.; Nethaji, M.; Chakravarty, A. R. *Inorg. Chem.* **2006**, *45*, 11043-11050.
[64]. Wang, Y.; Zhang, H.; Zhang, G.; Tao, W.; Tang, S. *J. Lumin.* **2007**, *126*, 211-218.
[65]. Dimiza, F.; Fountoulaki, S.; Papadopoulos, A. N.; Kontogiorgis, C. A.; Tangoulis, V.; Raptopoulou, C. P.; Psycharis, V.; Terzis, A; Kessissoglou, D. P.; Psomas, G. *Dalton Trans.* **2011**, *40*, 8555-8568.
[66]. Dimiza, F.; Papadopoulos, A. N.; Tangoulis, V.; Psycharis, V.; Raptopoulou, C. P.; Kessissoglou, D. P.; Psomas, G. *Dalton Trans.* **2010**, *39*, 4517-4528.
[67]. Sathyanarayana, S.; Dabroniak, J. C.; Chaires, J. B. *Biochemistry* **1992**, *31*, 9319-9324.
[68]. Rajput, C.; Rutkaite, R.; Swanson, L.; Haq, I.; Thomas, J. A. *Chem. Eur. J.* **2006**, *12*, 4611-4619.
[69]. Raja, D. S.; Bhuvanesh, N. S. P.; Natarajan, K. *Eur. J. Med. Chem.* **2011**, *46*, 4584-4594.
[70]. Khan, N. H.; Pandya, N.; Prathap, K. J.; Kureshy, R. I.; Razi Abdi, S. H.; Mishra, S.; Bajaj, H. C. *Spectrochim. Acta A* **2011**, *81*, 199-208.